J. Chem. Eng. Data 1992, 37, 107–110

Compressed Liquid Densities and Saturation Densities of Chlorodifluoromethane (R22)

Dana R. Defibaugh* and Graham Morrison

Thermophysics Division, Chemical Science & Technology Laboratory, National Institute of Standards and Technology, Gaithersburg, Maryland 20899

Density measurements for liquid chlorodifluoromethane (R22) were made with a vibrating-tube densimeter. The data range from 0.444 to 1.334 g/cm^3 along 13 isotherms between 263 and 373 K and pressures between 1000 and 6200 kPa. The accuracy of the data is estimated to be ±0.05%, except in the near-critical region.

Introduction

As a study of the performance characteristics of a vibrating-tube densimeter, we have measured the density of liquid chlorodifluoromethane (R22) over a range of temperatures and pressures where there are little data published. Here we report measurements in the compressed liquid region along 13 isotherms between 263 and 373 K and between 1000 and 6200 kPa. The purity of the sample used was 99.90 wt % R22 (*1*, *2*).

Apparatus and Procedure

The apparatus for measuring compressed liquid densities, shown schematically in Figure 1, was constructed around a stainless steel vibrating-tube densimeter (Anton-PAAR Model DPR412Y) (*2*). The stainless steel tube was enclosed in a steel heat exchanger. The temperature was regulated by circulating a water/ethylene glycol mixture through the heat exchanger from an external temperature-controlled circulating bath. A platinum resistance thermometer monitored the temperature (IPTS-68) of the water/glycol exiting the heat exchanger. The entire densimeter unit was further enclosed in an insulated air bath.

Argon was used to pressurize the system. Pressures in the apparatus were kept above the vapor pressure of the sample fluid to ensure that it remained in the compressed liquid state. The fluid in the vibrating tube was isolated from the argon by a mercury manometer separator. The pressure of the argon was measured with a quartz pressure transducer.

Before a sample was loaded, the densimeter and all the tubing were washed with absolute ethanol and then acetone to ensure the removal of any residue from previous runs using the vibrating tube. This precautionary washing was included in our routine after residue was encountered with a material that underwent decomposition. After the washing was completed, the system was evacuated overnight and cooled to 273 K. Mercury was then drawn into the manometer separator sight tube and reservoirs. The sample was loaded into the apparatus by allowing vapor to condense into the vibrating tube and connecting lines while the valve joining the two parts of the separator was closed. The mercury level in the manometer sight tube was monitored closely when the argon pressure was raised and when the valve for the separator was opened. The mercury in the sight tube moved only slightly when all the fluid in the vibrating tube was in the liquid state. Once the densimeter was filled, pressures, temperatures, and densities were recorded automatically with an IBM PC (*2*) through IEEE-488 and RS-232 interfacing. Data were taken along both isothermal or isobaric paths.

Results

The output of the densimeter was the time in microseconds for 1500 oscillations of the tube. The densimeter had been calibrated by measuring its output under vacuum ($\approx 10^{-4}$ Torr) and after it was filled with distilled, degassed water. Pressures during the calibration ranged between ambient and 6500 kPa, and temperatures ranged between 273 and 373 K (IPTS-68). The output for water was correlated to densities from the *NBS–NRC Steam Tables* by Haar et al. (*3*) through the following equation:

$$\rho = \frac{A((\tau/\tau_0)^2 - 1)}{(1 + BT)(1 + CP) + (DTP) + (ET^2P) + (FT^2)} \qquad (1a)$$

where $A = 4.127\,672\,37$ g/cm^3; $B = 5.771\,428 \times 10^{-5}$ K^{-1}; $C = 2.122\,165 \times 10^{-7}$ kPa^{-1}; $D = 5.173\,691 \times 10^{-12}$ K^{-1} kPa^{-1}; $E = -5.227\,885 \times 10^{-14}$ K^{-2} kPa^{-1}; and $F = 1.452\,904 \times 10^{-10}$ K^{-2}. Here τ_0 is the period of the vibrating tube under vacuum and was given by the expression

$$\tau_0/\mu\text{s} = 66778123 + 1300.782(T/\text{K}) + 0.7726851(T/\text{K})^2 \qquad (1b)$$

and τ is the experimental period in microseconds.

Coefficient A is related to the mean density of the vibrating tube including the empty inner cavity. Coefficients B–F reflect the temperature and pressure dependence of the period. Small volume changes occur in the vibrating tube with changing pressures as a consequence of the mechanical elasticity of stainless steel, and expansion occurs with changes in temperature.

The densities used for the calibration of the densimeter with water are shown in Figure 2. The range of densities is quite narrow and was a source of concern in using this instrument. The data were collected at approximately 10 K intervals along isobars where the temperature steps were controlled by computer. The density of water is represented to ±0.02% by eq 1 except at the extremes of the temperature range. The deviations of the calibration function from the *Steam Tables* are shown in Figure 3.

R22 was studied in the instrument to test the accuracy of the calibration at densities significantly different from 1 g/cm^3. Measurements were made along isotherms at pressures from 1000 to 6200 kPa and temperatures between 263 and 373 K. These results, given in Table I and shown graphically in Figure 4, cover the density range from 0.444 to 1.334 g/cm^3. The temperatures (IPTS-68) are accurate to ±0.005 K. The pressures are accurate to ±0.5 kPa. These measurements are compared in Figures 5 and 6 to the correlation developed by the Japanese Association of Refrigeration (JAR) (*4*) and to data of Zander (*5*) and of Uematsu (*6*). In the compressed liquid phase, below the critical temperature (T_c = 369.3 K), our data agree with the JAR surface and with the reference data within the claimed accuracy of Zander's data (*5*). There is a slight

---

*To whom correspondence should be addressed.

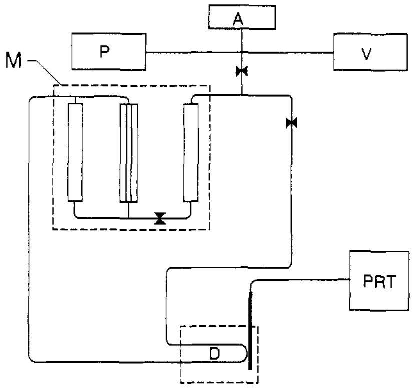

Figure 1. Schematic diagram of vibrating-tube densimeter apparatus: (A) argon pressure source; (P) quartz pressure range; (V) vacuum pump; (PRT) platinum resistence thermometer; (D) temperature-controlled water jacket enclosing vibrating tube; (M) mercury monometer separator reservoirs.

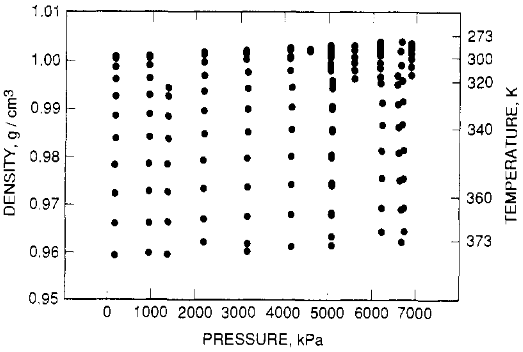

Figure 2. Compressed liquid density data for water between 273 and 373 K.

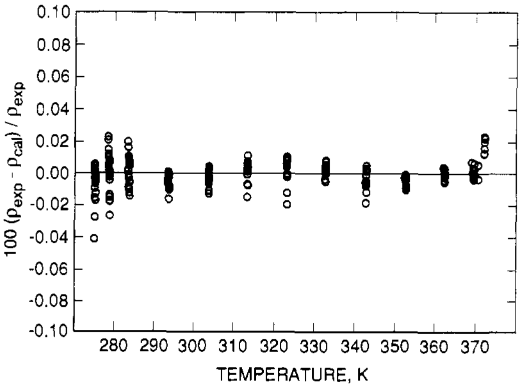

Figure 3. Differences plot between the calibration data and *NRC-NBS Steam Tables*.

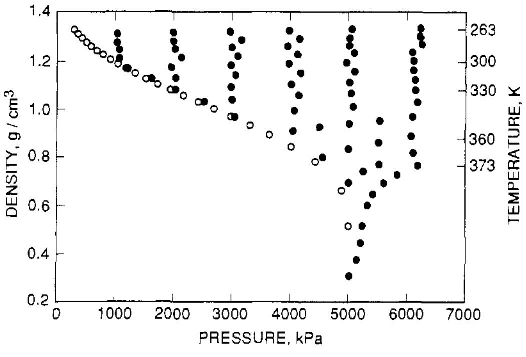

Figure 4. Compressed liquid density data for R22 between 263 and 373 K, data from Table I.

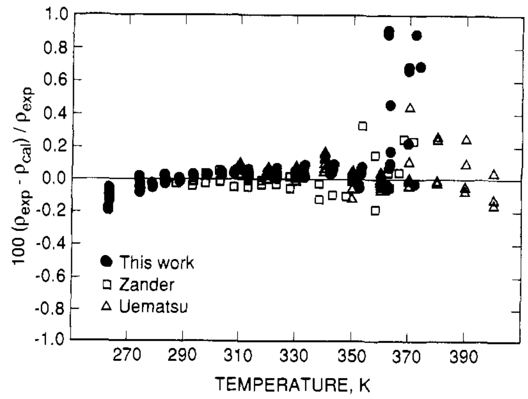

Figure 5. Deviation plot as a function of temperature between the correlation developed by the Japanese Association of Refrigeration and (●) this work, (□) Zander (*5*), and (△) Uematsu (*6*).

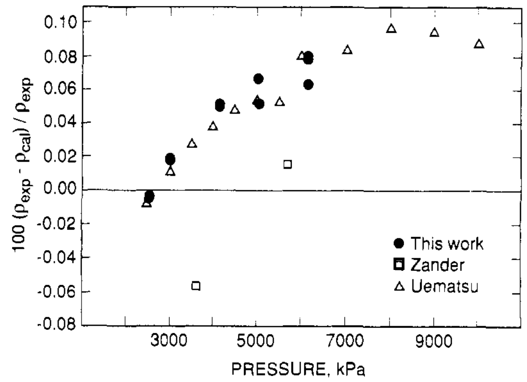

Figure 6. Deviation plot as a function of pressure between the Japanese Association of Refrigeration correlation (*4*) and (●) this work, (□) Zander (*5*), and (△) Uematsu (*6*).

tendency for Zander's densities to be lower than ours. Our measurements agree particularly well with the recent measurements of Uematsu (*6*). Near the critical point, the deviations from the JAR surface are as large as 2%. However, both Zander's and Uematsu's data show similar scatter. In this region, where small uncertainties in the temperature and pressure become important, we suspect that the vibration of the tube has an effect on the density of the fluid.

The saturated liquid densities given in Table II were obtained by extrapolating isotherms of compressed liquid to the saturation boundary. The saturation pressures were calculated from the following equation, modified from Goodwin and Haynes (*7*):

$$\ln (P/\text{kPa}) = A_1 T^{-1} + A_2 + A_3 T + A_4 (1 - T/T_c)^{1.5} \qquad (2)$$

where A_1 = -2907.443 K; A_2 = 17.05244; A_3 = -0.001796055 K^{-1}; A_4 = 2.204052; and T_c = 369.30 K. Coefficients A_1–A_4 were determined by McLinden (*8*). The extrapolation was carried out using a straight line through the two data points nearest the saturation boundary. This procedure works well so long as $T_c - T > 20$ K, where the isotherms are nearly linear. Near the critical temperature, the procedure produces high estimates of the saturation density because of the strong curvature in the isotherms. Our saturation densities were correlated by McLinden with the equation

$$\rho/\rho_c = 1 + D_1 r^{\beta} + D_2 r^{2/3} + D_3 r + D_4 r^{4/3} \qquad (3)$$

where $r = 1 - (T/T_c)$, T_c = 369.30 K; ρ_c = 0.513 g/cm^3; β = $^1/_3$; D_1 = 1.887739; D_2 = 0.5985853; D_3 = -0.071134; and D_4 = 0.4032765. Our values for the densities are in good agreement with Zander's, as shown in Figure 7. Below 333 K, our saturation densities are 0.05% higher than Zander's. This is consistent with the comparison of the two sets of com-

Table I. Experimental Data Collected by the Vibrating Tube Densimeter of R22

T/K	P/kPa	ρ/(g cm^{-3})	T/K	P/kPa	ρ/(g cm^{-3})	T/K	P/kPa	ρ/(g cm^{-3})	T/K	P/kPa	ρ/(g cm^{-3})
263.443	1045.4	1.3166	283.235	6248.6	1.2710	308.379	6255.5	1.1828	342.522	4242.4	1.0005
263.449	1045.7	1.3165	283.667	6250.3	1.2693	308.379	6256.0	1.1828	342.520	4242.5	1.0005
263.334	2001.3	1.3201	283.669	6250.3	1.2693	308.379	6256.2	1.1828	342.533	4242.8	1.0005
263.387	2011.1	1.3199	283.667	6250.4	1.2693	313.275	1634.8	1.1294	343.213	5066.1	1.0098
263.310	2987.6	1.3234	288.379	4783.7	1.2474	313.288	1634.8	1.1294	343.213	5067.7	1.0099
263.321	2992.5	1.3234	288.380	4787.8	1.2474	313.298	2042.6	1.1328	342.525	5210.8	1.0165
263.300	4001.7	1.3267	288.382	4792.2	1.2474	313.290	2042.7	1.1329	342.519	5211.2	1.0165
263.293	4001.8	1.3267	288.569	5099.6	1.2481	313.287	3070.3	1.1412	342.519	5211.8	1.0165
262.692	5056.8	1.3319	288.569	5099.8	1.2481	313.287	3070.4	1.1411	343.207	6170.0	1.0262
262.763	5059.3	1.3317	288.569	5099.8	1.2481	313.113	4169.4	1.1504	343.206	6182.4	1.0263
262.719	5061.0	1.3318	288.566	6251.0	1.2531	313.117	4169.5	1.1504	342.740	6184.9	1.0292
262.897	6235.6	1.3348	288.564	6251.1	1.2531	313.116	4169.7	1.1504	342.738	6185.0	1.0292
262.909	6236.3	1.3348	288.566	6251.3	1.2531	313.285	4186.6	1.1496	342.740	6185.7	1.0292
274.155	1036.0	1.2809	293.271	1077.2	1.2112	313.288	4186.7	1.1496	353.192	4066.2	0.9104
274.134	1036.3	1.2810	293.285	1077.4	1.2111	313.289	5107.2	1.1561	353.194	4066.7	0.9103
274.192	2004.6	1.2845	293.292	2136.4	1.2169	313.290	5109.2	1.1561	352.532	4274.0	0.9239
274.175	2005.1	1.2845	293.294	2137.0	1.2168	313.279	5127.3	1.1566	352.524	4274.7	0.9239
274.199	2005.2	1.2845	293.297	3109.7	1.2220	313.141	5127.8	1.1570	352.523	4275.1	0.9240
274.119	3172.3	1.2892	293.293	3109.8	1.2219	313.293	5128.1	1.1564	353.221	4497.8	0.9246
274.116	3172.3	1.2892	293.298	4136.7	1.2271	313.346	6116.0	1.1626	353.228	4498.9	0.9246
274.457	4089.5	1.2911	293.297	4137.0	1.2271	313.347	6116.0	1.1627	353.208	4511.9	0.9253
274.505	4090.1	1.2910	293.297	4137.3	1.2271	313.349	6116.3	1.1626	353.204	4512.8	0.9254
274.472	4090.5	1.2911	293.316	4698.6	1.2297	313.291	6118.4	1.1629	353.246	5018.4	0.9393
274.118	4168.0	0.2929	293.314	4703.2	1.2297	313.291	6118.8	1.1629	353.245	5018.5	0.9393
274.120	4168.3	1.2929	293.316	4707.5	1.2298	313.286	6120.7	1.1629	352.279	5252.5	0.9527
274.124	5024.2	1.2960	293.298	5090.1	1.2318	323.306	2030.7	1.0828	352.298	5252.6	0.9527
274.120	5025.0	1.2960	293.299	5029.4	1.2317	323.305	2032.7	1.0828	352.279	5253.1	0.9526
274.238	5059.7	1.2953	293.508	5110.6	1.2310	323.302	2034.6	1.0829	353.246	5526.1	0.9518
274.302	5065.7	1.2952	293.507	5110.8	1.2310	323.302	2999.9	1.0934	353.247	5526.8	0.9518
274.296	5069.9	1.2952	293.508	5111.1	1.2310	323.304	3001.2	1.0934	353.242	6094.9	0.9641
274.570	5073.3	1.2943	293.278	6098.4	1.2365	323.301	3001.6	1.0934	353.246	6097.4	0.9641
274.572	5073.3	1.2943	293.282	6099.8	1.2365	323.303	4025.3	1.1035	352.524	6220.3	0.9715
274.124	6225.9	1.3002	293.501	6256.5	1.2364	323.304	4026.0	1.1035	352.523	6220.7	0.9715
274.127	6226.7	1.3002	293.504	6257.1	1.2364	322.886	4181.4	1.1072	352.524	6221.2	0.9715
274.329	6267.0	1.2993	293.501	6257.6	1.2364	322.883	4185.4	1.1072	362.196	4327.7	0.7976
274.275	6268.4	1.2995	298.463	4615.2	1.2107	322.884	4187.0	1.1071	362.197	4327.8	0.7975
274.274	6268.5	1.2995	298.460	4619.2	1.2107	323.300	5018.7	1.1125	362.197	4328.6	0.7975
278.507	4098.1	1.2779	298.450	4623.6	1.2108	323.302	5019.3	1.1125	363.218	4565.4	0.7991
278.627	4098.2	1.2776	298.489	5121.0	1.2132	322.789	5154.2	1.1161	363.219	4567.4	0.7993
278.522	4098.3	1.2778	298.490	5121.0	1.2132	322.788	5154.3	1.1162	363.225	5003.2	0.8353
278.610	4968.3	1.2809	298.491	5121.0	1.2132	322.787	5154.3	1.1162	363.224	5003.4	0.8353
278.618	4973.1	1.2809	298.486	6258.6	1.2190	323.112	6133.7	1.1228	362.128	5301.4	0.8649
278.622	4977.0	1.2809	298.486	6258.9	1.2190	323.112	6134.4	1.1228	362.133	5302.5	0.8649
278.766	5081.0	1.2808	298.485	6259.5	1.2190	323.113	6135.0	1.1228	362.131	5302.6	0.8650
278.765	5081.1	1.2808	303.493	1219.2	1.1704	323.299	6152.9	1.1220	363.225	5510.2	0.8628
278.767	5081.2	1.2808	303.495	1219.4	1.1703	323.297	6153.5	1.1220	363.227	5512.1	0.8629
278.606	6259.7	1.2857	303.494	1971.6	1.1754	333.147	2537.0	1.0322	363.233	6083.8	0.8857
278.599	6261.4	1.2857	303.485	1972.8	1.1756	333.148	2537.2	1.0322	363.233	6085.4	0.8858
278.608	6262.3	1.2857	303.459	3001.2	1.1823	333.151	3016.0	1.0395	362.151	6258.8	0.9010
283.226	1072.1	1.2490	303.473	3004.1	1.1822	333.146	3016.5	1.0395	362.148	6259.3	0.9010
283.220	1072.4	1.2489	303.431	3994.4	1.1885	333.155	4155.7	1.0549	362.155	6259.9	0.9010
283.220	2031.0	1.2534	303.440	3995.5	1.1884	333.152	4157.2	1.0549	372.025	4610.5	0.2386
283.221	2031.5	1.2533	303.265	4534.8	1.1922	332.685	4211.3	1.0583	372.025	4610.7	0.2387
283.223	2031.9	1.2533	303.269	4538.0	1.1922	332.683	4211.5	1.0584	372.023	4610.9	0.2387
283.221	3017.1	1.2577	303.266	4542.1	1.1922	332.690	4211.7	1.0583	369.658	5015.2	0.6940
283.221	3018.1	1.2577	303.421	4970.3	1.1943	333.156	5037.3	1.0652	369.666	5017.7	0.6945
283.222	3974.8	1.2618	303.422	4971.6	1.1942	333.154	5037.3	1.0654	369.649	5253.2	0.7387
283.223	3975.1	1.2617	303.486	5130.9	1.1947	333.154	5040.6	1.0654	369.649	5254.9	0.7390
283.417	4106.7	1.2614	303.487	5131.0	1.1947	332.484	5180.6	1.0706	372.154	5390.1	0.6940
283.418	4107.1	1.2614	303.486	5131.1	1.1947	332.551	5181.5	1.0705	372.186	5392.5	0.6908
283.449	4107.4	1.2612	303.394	6122.5	1.2008	332.483	5182.9	1.0707	372.193	5393.1	0.6894
283.545	4872.9	1.2641	303.409	6122.9	1.2006	333.154	6141.9	1.0722	369.647	5521.1	0.7716
283.559	4877.8	1.2641	303.482	6257.3	1.2010	333.155	6134.4	1.0771	369.642	5521.8	0.7716
283.684	4882.6	1.2638	303.481	6257.4	1.2010	333.153	6145.1	1.0773	369.639	6111.6	0.8179
283.217	5008.4	1.2660	303.481	6258.3	1.2010	332.803	6158.0	1.0794	369.644	6113.3	0.8180
283.220	5009.5	1.2660	308.238	4455.6	1.1722	332.802	6158.6	1.0794	372.167	6325.2	0.7968
283.249	5023.4	1.2661	308.266	4459.9	1.1722	332.801	6159.0	1.0794	372.169	6325.2	0.7967
283.687	5088.7	1.2646	308.275	4462.5	1.1722	343.212	3068.4	0.9709	372.171	6325.9	0.7967
283.685	5088.8	1.2646	308.388	5141.1	1.1760	343.213	3069.0	0.9709			
283.687	5089.9	1.2646	308.387	5141.1	1.1760	343.215	4071.0	0.9925			
283.240	6247.7	1.2710	308.386	5141.1	1.1760	343.214	4073.2	0.9925			

pressed liquid data. Except for the 363 K measurement, our data fall within the scatter of Zander's measurements above 333 K. Our determination at 363 K is higher than that of Zander because of the curvature of the near-critical isotherm.

Discussion

Our motivation in these measurements was to test the range over which one could expect the vibrating-tube instrument to

Table II. Saturated Liquid Densities for R22

T/K	P/kPa	ρ/(g cm^{-3})	T/K	P/kPa	ρ/(g cm^{-3})
263.443	423.2	1.3142	323.300	1948.7	1.0816
274.155	514.9	1.2786	333.150	2426.1	1.0304
283.220	682.8	1.2467	343.210	3001.6	0.9695
293.280	913.5	1.2098	353.190	3668.9	0.8939
303.500	1202.6	1.1698	363.220	4451.3	0.7806
313.290	1538.3	1.1282			

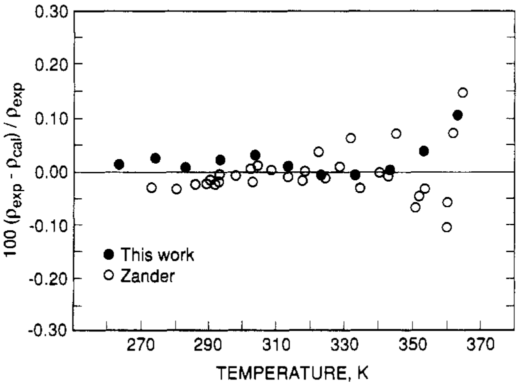

Figure 7. Deviation plot as a function of temperature of saturated liquid densities of (●) this work and (○) Zander (*5*), from eq 3.

work with a limited range of calibration densities. The output of the instrument was correlated with water, which has a density of nearly 1 g/cm^3 throughout our temperature range. Our correlation achieved a precision of ±0.02% in density. Our measurements on R22 show that the instrument can measure fluids of considerably different densities with similar accuracy. In showing this, we also expanded the data on R22, obtaining good agreement with the recent Uematsu data. We also found a regular pattern in departures from the JAR representation.

Acknowledgment

We thank John S. Gallagher for providing software for the correlation of water and Racon Inc. for providing information on the R22 purity.

Registry No. R22, 75-45-6.

Literature Cited

(1) R22 obtained from Racon Inc., Wichita, KS, purity data by private communication.
(2) Brand names and commercial sources of materials and instruments, when noted, are given for scientific completeness. Such information does not constitute a recommendation by the National Institute of Standards and Technology nor does it suggest that these products or instruments are the best for the described application.
(3) Harr, L.; Gallagher, J.; Kell, G. *NBS/NRC Steam Tables*; Hemisphere Publishing Corp.: New York, 1984.
(4) Japanese Association of Refrigeration. *Thermophysical Properties of Refrigerants: R22 Chlorodifluoromethane*; Japanese Association of Refrigeration: Tokyo, Japan, 1975.
(5) Zander, M. *Proc. 4th Symp. Thermophys. Prop. Gases, Liq., Solids, ASME*, **1968**, 114.
(6) Fukuizumi, H.; Uematsu, M. *J. Chem. Eng. Data* **1991**, *36*, 91-93.
(7) Goodwin, R. D.; Haynes, W. M. *Thermophysical properties of isobutane from 114 to 700 K at pressures to 70 MPa*; National Bureau of Standards Technical Note 1051; U.S. Government Printing Office: Washington, DC, 1982.
(8) McLinden, M. O. Thermodynamic Properties of CFC Alternatives: A Survey of Available Data. *Int. J. Refrig.* **1990**, *13*, 149.

Received for review May 9, 1991. Accepted October 10, 1991.

Refractive Indexes of Aqueous LiBr Solutions

Abdolreza Zaltash and Moonis R. Ally*

Energy Division, Oak Ridge National Laboratory, P.O. Box 2008, Building 3147, MS 6070, Oak Ridge, Tennessee 37831-6070

The refractive indexes of water–lithium bromide solutions were measured in the temperature range from 5.0 to 80.0 °C and in the range of salt concentrations from 0.00 (deionized water) to 58.90 mass %. An electrolyte solution of LiBr in water was chosen for study because of its wide use as an absorption chiller fluid. The concentration of LiBr aqueous solution was determined by argentimetric titration using tetrabromofluorescein (Eosin) as an adsorption indicator and was checked at a few discrete concentrations (10.06, 20.30, and 58.90 mass % LiBr) against the values obtained by gravimetric analysis. The deviation between values obtained using these two techniques was found to be less than 0.27 mass %. The refractive indexes are shown to represent a reliable and convenient way of measuring the concentration of salt (or water) in LiBr solutions with accuracies of ±0.3 mass % salt.

Introduction

Water–lithium bromide solutions are being used in absorption chillers, absorption heat transformers, and absorption refrigerating machines (*1–3*). In testing of a prototype absorption machine, it is necessary to obtain the solution concentration at various locations as a function of temperature and time. The technique of withdrawing a sample for refractive index measurement or measuring the refractive index in situ (*4*) is a reliable and convenient method of concentration measurement. Unfortunately, the available data on refractive index of LiBr appears limited to 25 °C (*5*, *6*). The scope of this paper deals with measurements of refractive indexes of LiBr solutions as a function of salt concentration and temperature and their reliability as a method for determining solute concentrations.

Experimental Apparatus and Technique

An Abbe-3L refractometer (Milton Roy Co., Type 33-46-10) connected to a constant-temperature circulating bath (VWR, Model 1145, LED set/read circuitry) was used for refractive index measurements. Refractive indexes at discrete salt concentrations and temperatures were determined. The concentration of LiBr in aqueous solutions was determined by argentimetric titration (*7*) using tetrabromofluorescein (Eosin, J. T. Baker Chemical Co., lot no. 546712) as an adsorption indicator. LiBr salt was supplied by EM Science (GR, extra pure; LX0320-6).

Solutions were filtered to remove trace amounts of insoluble impurities. The titrimetric analysis for salt concentration (mass

---

* To whom all correspondence should be addressed.

0021-9568/92/1737-0110$03.00/0